

Selective Area Synthesis of Magnesium Oxide Nanowires

G. B. Thompson – The University of Alabama  
et al.

Deposited 11/12/2018

Citation of published version:

Kim, G., et al. (2007): Selective Area Synthesis of Magnesium Oxide Nanowires. *Journal of Applied Physics*, 102(10). DOI: <https://doi.org/10.1063/1.2817259>

## Selective area synthesis of magnesium oxide nanowires

G. Kim, R. L. Martens, G. B. Thompson, B. C. Kim, and A. Gupta<sup>a)</sup>

*Center for Materials for Information Technology, The University of Alabama,  
Tuscaloosa, Alabama 35487-0209, USA*

(Received 27 July 2007; accepted 25 September 2007; published online 28 November 2007)

Single crystalline magnesium oxide (MgO) nanowires exhibiting a square cross section have been grown on (001)-oriented MgO and Si substrates using the vapor-liquid-solid growth mechanism. While the nanowires grow vertically aligned on MgO, they display random orientations on the silicon substrate. For growth on MgO substrates, the selective placement and density of the nanowires can be controlled by using electron beam lithography for pre patterning the gold catalyst layer. The nanowire samples have been characterized using field-emission scanning electron microscopy and transmission electron microscopy. The described process for selective placement of the nanowires is attractive for their use as templates for coaxial coatings and also for their manipulation for potential device fabrication. © 2007 American Institute of Physics. [DOI: 10.1063/1.2817259]

### I. INTRODUCTION

Nanowires represent an important class of one-dimensional structures that are attractive for a wide range of potential applications in consumer electronics, biomedicine, and optoelectronics and for the defense industry.<sup>1-4</sup> Toward these goals, numerous methods have been investigated for the synthesis of nanowire materials such as ZnO, MgO, Si, and GaN, and their properties are studied in detail.<sup>5-8</sup> Besides the use for their unique intrinsic properties, the nanowires can be utilized as an inert template for the growth of “core/shell” coaxial heterostructures of a variety of other materials, thereby increasing their functionality.<sup>9</sup> Such coaxial structures can be fabricated by coating an array of synthesized nanowire templates with conformal layers of some other functional material, such as ferroelectric or ferromagnetic oxides. It is important that the chosen coating method provides excellent uniformity and control of the sheath thickness. The formation of coaxial structures is still in its infancy since it requires the controlled growth in both the position and density of the nanowires in order to reduce the shadowing effect during deposition of the coating and also for subsequent device fabrication and integration.

Magnesium oxide (MgO) is an attractive material for use as a nanowire template because of its thermal stability, chemical inertness, and excellent electrical insulating characteristics.<sup>6,10</sup> Han *et al.*<sup>11</sup> have reported the growth of vertically aligned MgO nanowires by utilizing the vapor-liquid-solid (VLS) growth mechanism with Mg<sub>3</sub>N<sub>2</sub> as a precursor.<sup>12</sup> A high density array of nanowires is produced using a blanket gold thin film as a catalyst with this relatively simple chemical vapor deposition (CVD) process. However, the random placement of the nanowires with high density is a challenge for the subsequent functionalization and selective placement of the nanowires. More recently, Kawai and co-workers have used the pulsed laser deposition (PLD) tech-

nique for the growth of MgO nanowires using gold catalyst and have studied in detail the effects of temperature, ambient pressure, and ablated particle flux on the growth rate and morphology of the synthesized wires.<sup>13</sup>

In this paper, we report on the details regarding the MgO nanowire growth process using CVD. We further demonstrate control of the growth in selected areas by patterned deposition of the gold catalyst layer. The vertically grown nanowires at preselected positions are attractive for use as template posts for coating of thin films and also for their manipulation to fabricate nanodevice structures. We have grown single crystalline MgO nanowires with a square cross section both on Si (001) and MgO (001) substrates. A good correlation is observed between the density, average diameter, and distribution of the nanowires with those of the initial gold catalyst islands formed at the deposition temperature. Unlike growth with random orientations and sizes on Si, the nanowires grow vertically on the MgO substrate and exhibit a much more uniform size and shape distribution. The latter appear particularly promising for the selective growth of nanowires in prepatterned regions using electron beam lithography.

### II. EXPERIMENT

The MgO nanowires are synthesized on (001)-orientated single crystalline MgO and Si substrates utilizing the VLS growth mechanism with gold as a catalyst.<sup>12</sup> We employed two methods for the gold particle formation—a random arrangement, used to optimize the process conditions for the growth of the nanowires, and a systematic pattern array formation using electron beam lithography.

For both the random arrangement and patterned methods, an ~1 nm thin gold film is electron beam evaporated onto the MgO and Si substrates. For patterning the gold layer, a negative e-beam resist (Fox-12) is then spin coated onto the substrate surface. The resist-coated substrate is next transferred to a JEOL-7000F FEG-scanning electron microscope (SEM), equipped with Nabity electron beam lithogra-

<sup>a)</sup>Author to whom correspondence should be addressed. Electronic mail: agupta@mint.ua.edu

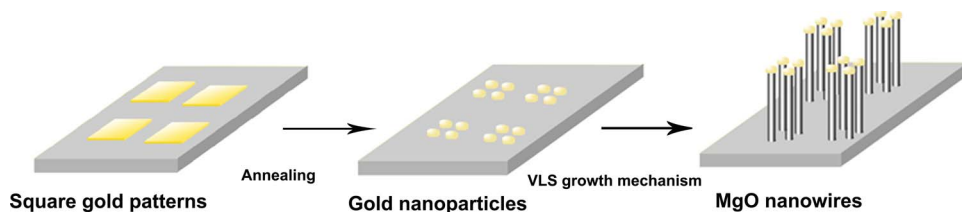


FIG. 1. (Color online) Schematic diagram illustrating the growth sequence of MgO nanowires. The square gold regions are patterned using e-beam lithography.

phy patterning capability, to pattern three different square arrays of dimensions of 0.25, 1, and 4  $\mu\text{m}^2$ . Postpatterning, the substrates are ion milled to remove the gold thin film in all areas except for the patterned regions. Final lift-off of the resist on top of the gold in the patterned regions is accomplished using dilute HF (<1%), followed by isopropanol and de-ionized water rinse and drying.

Both the continuous coverage and patterned gold film coated substrates are then transferred into a horizontal quartz-tube furnace, which is heated up to 925  $^\circ\text{C}$  under a constant argon flow rate of 100 SCCM (SCCM denotes cubic centimeter per minute at STP). At this high temperature, the continuous film transforms to a discontinuous array of semicircular-shaped nanometer-sized particles because of the overall reduction of the surface tension. These particles form the catalytic sites for the growth of the nanowires in the presence of suitable reactant species. By selectively patterning the gold film, the nanoparticles are confined to specific regions on the substrate. After cooling the substrates to room temperature in the furnace, they are removed and the nanoparticles are characterized by SEM.

After characterization, the substrates are placed back into the tube furnace along with the magnesium nitride ( $\text{Mg}_3\text{N}_2$ ) powder precursor to synthesize the MgO nanowires. A fixed flow rate of 100 SCCM ultrapure argon gas is mixed with a 60 SCCM flow of Ar/0.02%  $\text{O}_2$  mixture and together introduced into the furnace at atmospheric pressure. The furnace temperature is then raised to 925  $^\circ\text{C}$ , whereby  $\text{Mg}_3\text{N}_2$  volatilizes and decomposes into its constituent elements. Argon acts as a carrier gas to transfer the elemental magnesium produced by decomposition onto the gold catalyst covered substrates for the growth of the MgO nanowires by oxidation, as shown in the schematic diagram of Fig. 1. It is important to maintain a very low concentration of oxygen during the growth process in order to prevent vapor-phase nucleation and growth of MgO particles. After the completion of the nanowire synthesis, the furnace tube is slowly cooled down to room temperature under a constant flow of argon.

The structure and density of the nanowires have been characterized using a field-emission JEOL 7000F SEM and a FEI Tecnai F20 200 keV transmission electron microscope (TEM). The nanowires are mechanically removed from the substrate by scraping and collected onto an electron transparent carbon coated grid for the TEM analysis.

### III. RESULTS AND DISCUSSION

The random array of gold nanoparticles generated on the surface of MgO and Si substrates on heating, along with the subsequent growth of nanowires on these surfaces, generates two distinct morphologies, as seen in Fig. 2. The nanowires

grow vertically off from the MgO substrate. In contrast, the NWs on the Si substrate form a “basket-weave-like” morphology, being intertwined and at various nonvertical growth directions. The inset images of Fig. 2 show the morphology and density of gold nanoparticles, which act as the catalyst for the VLS growth mechanism of the MgO nanowires. The average length of the MgO nanowire grown on the MgO substrate is  $\sim 1 \mu\text{m}$  for a deposition period of 60 min. On the other hand, the nanowires grown for the same time period on Si substrate are significantly longer, as seen in Fig. 2.

The overall reaction leading to the formation of the MgO nanowires from the precursor can be represented by the chemical reaction

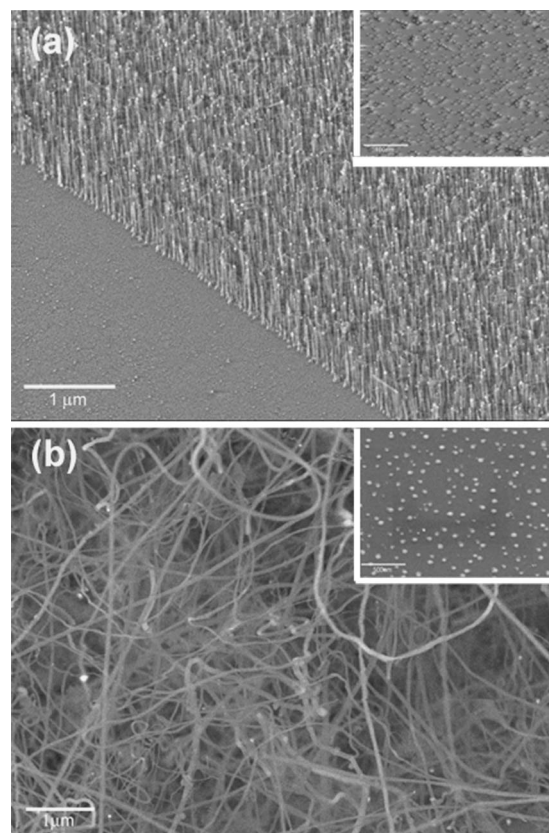
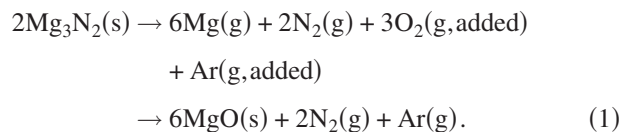


FIG. 2. (a) SEM images showing the growth of vertically aligned MgO nanowires on a (001)-oriented MgO substrate for a total deposition period of 60 min. The inset shows an image of the gold particles formed by heating the gold film on the MgO substrate to the growth temperature and then cooled down without actual growth of the nanowires. (b) SEM image showing MgO nanowires grown on a (001)-oriented Si substrate for a total deposition period of 60 min. The wires grow in random directions exhibiting a basket-weave-like morphology. The inset shows the gold particles formed by heating the gold film on the Si substrate to the growth temperature and then cooled down without actual growth of the nanowires. The marker for both inset images is 100 nm.



The small added concentration of oxygen with the argon carrier gas is likely adsorbed on the surface of the gold catalyst and reacts with the magnesium vapor to form the initial nuclei that result in the growth of MgO nanowires. For Si nanowires, Kodambaka *et al.*<sup>14</sup> have reported that the ambient oxygen concentration reduces the gold diffusion along the sidewalls during growth process, enabling the nanowire to grow longer and have an untapered geometry. On the other hand,

Yanagida *et al.*,<sup>13</sup> based on their MgO nanowire growth experiments using PLD, have suggested that the total ambient pressure (either argon or oxygen) and not the actual oxygen content which gets incorporated into the MgO nanowires is critical for enhancing the growth. Nonetheless, they observed that the oxygen concentration is critical for the degree of crystallinity of the MgO nanowires. The gold nanoparticle usually “rides” atop the growing structure and its size remains essentially unchanged during the entire process of the nanowire growth, as has been previously observed in other VLS grown structures.<sup>15</sup> However, under nonoptimal growth conditions, the gold catalyst can diffuse away during growth and the wire’s height can be shunted.<sup>13</sup> The SEM images of Fig. 2 do show gold particles at the tip of the longer wires indicating limited gold catalyst diffusion away from the tip of the nanowire under our operating conditions. TEM images and diffraction patterns, shown in Fig. 3, indicate that the nanowires have a rectangular cross section with the  $\langle 001 \rangle$  growth direction. This growth direction is to be expected based on the homoepitaxy that occurs between the MgO nanowire and the MgO (001) substrate at these processing temperatures. Unlike the MgO substrate, the nanowires are not epitaxially anchored onto the (001) Si substrate. Moreover, a pristine Si surface is not present during the growth since the partial pressure of oxygen, particularly at these processing temperatures, will enhance the natural oxidation of the Si surface. As the MgO nanowires nucleate and grow in length, the lowest surface energy facets will dominate and preferentially grow in whichever direction they are formed. All the nanowires grown to different heights and on different substrates, exhibit the square rod shape. In general, the  $\{001\}$  facets in rock-salt crystals, such as MgO, have the lowest surface energy,<sup>16</sup> allowing the nanowires to maintain the cubic shape facets perpendicular to the axial growth direction of the nanowires on the MgO substrate. In contrast, since the nucleation of nanowires is not fixed to any particular direction from the Si substrate, as Colli *et al.*<sup>17</sup> have reported for ZnO nanowires on Si, they grow outwardly in multiple directions and develop the basket-weave morphology.

The nanowires’ cube length of the rectangular wires, termed “diameter,” has been measured from the TEM images. A comparison of the nanowire diameters in Fig. 4 shows that the average diameters are  $29 \pm 13$  and  $19 \pm 5$  nm for the Si and MgO substrates, respectively. Additionally, the Si substrate shows a greater wire-to-wire diameter variability

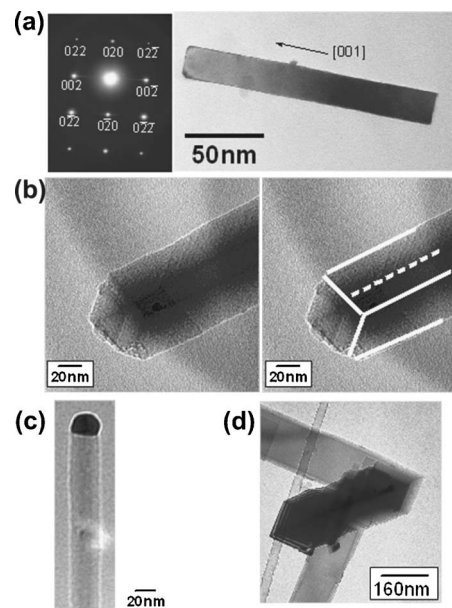


FIG. 3. (a) TEM diffraction pattern and bright field image of a single MgO nanowire grown on the MgO substrate indicating a  $\langle 001 \rangle$  growth direction. (b) MgO nanowire showing the cubic-rod shape morphology; the image to the right has the cube edges highlighted. (c) TEM bright field image of a MgO nanowire with the gold catalyst on top, which has been grown on an MgO substrate. (d) TEM bright field image of MgO nanowires grown from the Si substrate. Note the rectangular shape of the nanowires and interconnection of the wires to each other in different directions. This type of interconnection was not evident in the MgO nanowires grown on the MgO substrate.

ity. A histogram comparing the initial gold particle sizes between the two substrates is plotted in Fig. 5. The average gold particles’ diameters were found to be  $51 \pm 11$  and  $23 \pm 7$  nm for the Si and MgO substrates, respectively. Similar to the wire variability, the Si substrate gold particles show a greater range in sizes. This is likely because of differences in the surface tension between liquid Au–Si and liquid Au–

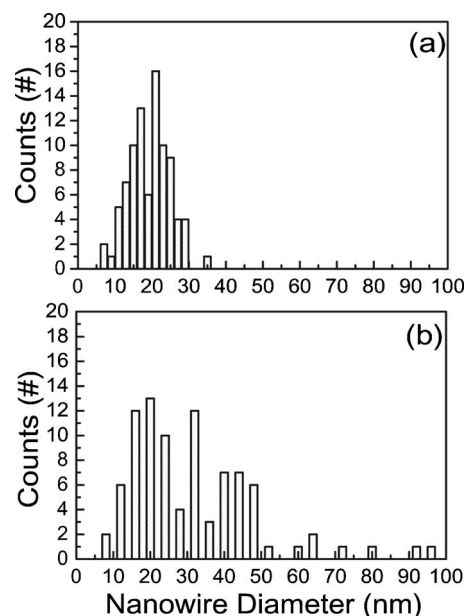


FIG. 4. Histograms comparing the diameter of MgO nanowires grown on (a) MgO (001) and (b) Si (001) substrates.

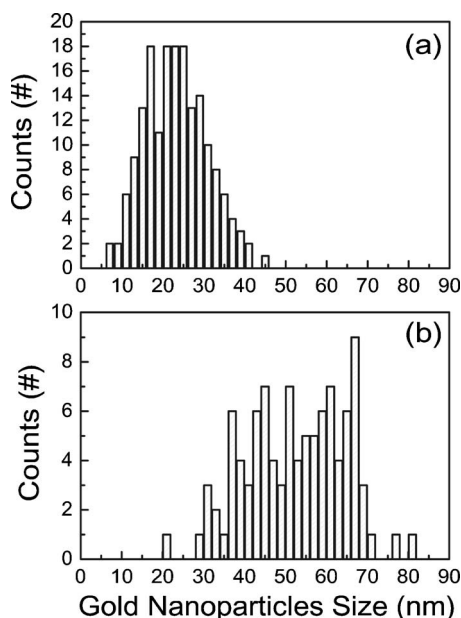


FIG. 5. Histograms comparing the size of gold nanoparticles formed using an  $\sim 1$  nm gold film on (a) MgO (001) and (b) Si (001) substrates.

MgO interfaces. Metal films grown on oxide surfaces are known to significantly “ball up” because of the high surface tension.<sup>18</sup> By providing thermal energy, as in our growth process, the metal surface mobility is enhanced, resulting in both the driving force and mobility to produce small metal particles on the oxide surface that have little variability in the contact angle. The larger average size and larger range of sizes of the gold catalysis particles invariably contribute to the variability in the nanowire diameters. Additionally, the random basket-weave morphology of the nanowires on the Si substrate will hinder uniform growth because of the tortuous diffusion path for transporting the precursors to the growing wires. Collectively, this will contribute to different growth rates for each nanowire depending on its location. In contrast, the nearly uniform gold catalyst sizes and vertical growth direction of the nanowires from the MgO substrate provide for more consistent growth conditions and reduced variability in the final nanowire sizes. Additionally, for MgO substrate nanowires, there is no appreciable diameter varia-

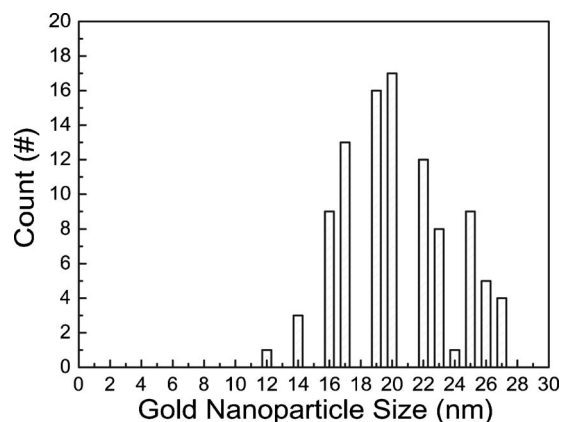


FIG. 7. Histogram of the size distribution of gold nanoparticles formed within the  $1 \mu\text{m}^2$  patterned regions on an MgO (001) substrate. The average nanoparticle size is 20 nm.

tion along the  $\sim 1 \mu\text{m}$  axial length of the nanowires. Based on the random array results, we have ruled out Si as an adequate substrate for selectively patterning well-ordered nanowire arrays. The selective patterning has thus only been performed on the MgO (100) substrates.

Following the procedures described in Sec. II, a series of gold catalysis regions has been selectively patterned into different regions of  $0.25$ ,  $1$ , and  $4 \mu\text{m}^2$ . The SEM images, shown in Figs. 6(a)–6(c), depict a different number of free-standing MgO nanowires grown in the various gold pattern regions, respectively. The regions over which the wires grow are approximately 50% larger than the initially patterned square areas. At  $925^\circ\text{C}$ , the liquidlike gold layer has an enhanced mobility and is likely to spread out and extend beyond the patterned areas. A histogram comparing the gold nanoparticle sizes formed at the reaction temperature in a patterned region of  $1 \mu\text{m}^2$  is shown in Fig. 7 (measured after cooling to room temperature). The properties of patterned nanowires are summarized in Table I. For each patterned region, the nanowires exhibit a fairly good uniformity in both size and quantity. Additionally, changing the size of the pattern area does not appear to dramatically alter the nanowire sizes or packing density between the different regions studied. The ability to selectively pattern nanowires into spe-

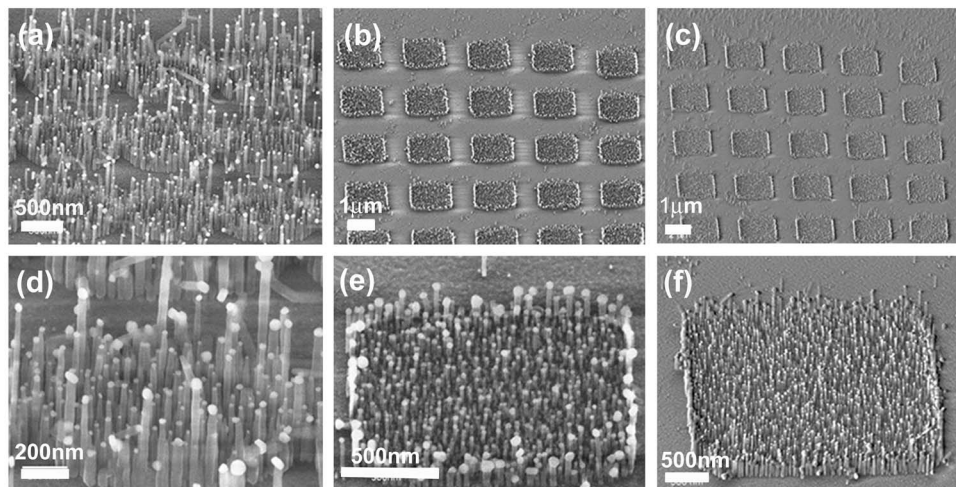


FIG. 6. SEM images showing different patterned regions of the MgO nanowires. The bright spot on the top of each nanowire is the gold catalyst particle. [(a) and (d)]  $0.25 \mu\text{m}^2$ , [(b) and (e)]  $1 \mu\text{m}^2$ , and [(c) and (f)]  $4 \mu\text{m}^2$ . A blanket gold film of  $\sim 1$  nm thickness is deposited and patterned using e-beam lithography for the selective growth of the nanowires.

TABLE I. Tabulation of the absolute number and density of the grown nanowires, along with the number of gold catalyst particles formed at the growth temperature, for the different lithographically patterned areas.

Measured square areas ( $\mu\text{m}^2$ )	0.55	1.5	6.4
Number of nanowires	124	297	1092
Density of nanowires ( $\mu\text{m}^{-2}$ )	225	198	170
Size of gold nanoparticles (nm)	$19\pm 4.9$	$20.4\pm 7.2$	$18.4\pm 4.2$

cific locations and control the shape, size, and density provide the ability to functionalize and manipulate these structures for the fabrication of nanoscale devices.

#### IV. CONCLUSION

MgO nanowires with a square cross section have been successfully synthesized using the VLS method. Depending on the substrate and placement of the gold catalyst, the nanowires can have uniform diameter and display position-controlled growth. The size variability of the nanowires can be directly correlated with the variability in the size of the gold catalyst particles and the extent of uniformity in the growth morphology. The MgO nanowires grow homoepitaxially normal to the MgO substrate, whereas the nanowires grown on the Si substrate exhibit a variety of different growth directions even though they are all single crystalline. On both MgO and Si, the nanowires exhibit a  $\langle 001 \rangle$  growth direction, as determined using TEM. Using e-beam lithography, selective synthesis of MgO nanowires has been achieved with control on both the size and density of the nanowires. Upon annealing the patterned gold film to the growth temperature of the nanowires, the patterned regions expand beyond the original dimensions but reasonably maintain the original shape. The patterning and growth of MgO nanowires, with control on their placement, are attractive for their use as template posts for functionalization and for device fabrication and integration.

#### ACKNOWLEDGMENTS

The work has been supported by NSF Grant No. ECS-0609388 and NSF MRSEC Grant No. DMR-0213985. The Tecnai TEM used for the nanowire characterization was acquired through the National Science Foundation Major Instrumentation Program Grant No. DMR-0421376.

- <sup>1</sup>Z. Zhong, D. Wang, Y. Cui, M. W. Bockrath, and C. M. Lieber, *Science* **302**, 1377 (2003).
- <sup>2</sup>G. Zheng, F. Patolsky, Y. Cui, W. U. Wang, and C. M. Lieber, *Nat. Biotechnol.* **23**, 1294 (2005).
- <sup>3</sup>X. Wang, C. J. Summers, and Z. L. Wang, *Nano Lett.* **4**, 423 (2004).
- <sup>4</sup>L. Luoa, Y. Zhang, S. S. Maob, and L. Lin, *Sens. Actuators, A* **127**, 201 (2006).
- <sup>5</sup>Z. L. Wang and J. Song, *Science* **312**, 242 (2006).
- <sup>6</sup>R. Ma and Y. Bando, *Chem. Phys. Lett.* **370**, 770 (2003).
- <sup>7</sup>W. Y. Yee, M. Yahaya, M. M. Salleh, and B. Y. Majlis, *IEEE-ICSE*, 2004 (unpublished), p. 379.
- <sup>8</sup>T. Kukendall, P. J. Pauzaskie, Y. Zhang, J. Goldberger, D. Sirbully, J. Denlinger, and P. Yang, *Nat. Mater.* **3**, 524 (2004).
- <sup>9</sup>W. Lu and C. M. Lieber, *J. Phys. D* **39**, R387 (2006).
- <sup>10</sup>P. Yang and C. M. Lieber, *J. Mater. Res.* **12**, 2981 (1997).
- <sup>11</sup>S. Han, C. Li, Z. Liu, B. Lei, D. Zhang, W. Jin, X. Liu, T. Tang, and C. Zhou, *Nano Lett.* **4**, 1241 (2004).
- <sup>12</sup>R. S. Wagner and W. C. Ellis, *Appl. Phys. Lett.* **4**, 89 (1964).
- <sup>13</sup>T. Yanagida, K. Nagashima, H. Tanaka, and T. Kawai, *Appl. Phys. Lett.* **91**, 061502 (2007); A. Marcu, T. Yanadiga, K. Nagashima, H. Tanaka, and T. Kawai, *J. Appl. Phys.* **102**, 016102 (2007); K. Nagashima, T. Yandiga, H. Tanaka, and T. Kawai, *Appl. Phys. Lett.* **90**, 233103 (2007); K. Nagashima, T. Yanadiga, H. Tanaka, and T. Kawai, *J. Appl. Phys.* **101**, 124304 (2007).
- <sup>14</sup>S. Kodambaka, J. B. Hannon, R. M. Tromp, and F. M. Ross, *Nano Lett.* **6**, 1292 (2006).
- <sup>15</sup>For example, see Y. Xia, P. Yang, Y. Sun, Y. Wu, B. Mayers, B. Gates, Y. Yin, F. Kim, and H. Yan, *Adv. Mater. (Weinheim, Ger.)* **15**, 353 (2003), and references therein.
- <sup>16</sup>E. G. Wolff and T. D. Coskren, *J. Am. Ceram. Soc.* **48**, 279 (1965).
- <sup>17</sup>A. Colli, A. Fasoli, P. Beecher, P. Servati, S. Pisana, Y. Fu, A. J. Flewitt, W. I. Milne, and J. Robertson, *J. Appl. Phys.* **102**, 034302 (2007).
- <sup>18</sup>C. T. Campbell, *Surf. Sci. Rep.* **27**, 1 (1997).